Phase Separation of Binary Polymer Mixtures under an Electric Field

Hironobu Hori,[†] Osamu Urakawa,*,[‡] Okimichi Yano, and Qui Tran-Cong-Miyata

Department of Macromolecular Science and Engineering, Graduate School of Science and Technology, Kyoto Institute of Technology, Matsugasaki, Sakyo-ku, Kyoto 606-8585, Japan

Received September 8, 2006; Revised Manuscript Received November 9, 2006

ABSTRACT: Time evolution of phase separation under an AC electric field was studied for poly(2-chlorostyrene)/ poly(vinyl methyl ether) blends containing 0.5 wt % lithium perchlorate ($LiClO_4$) near the critical point. We observed anisotropic morphologies with the interfaces aligned parallel to the direction of the field between two electrodes. The degree of anisotropy (D) was quantitatively evaluated by image analysis of the resulting morphology observed with an optical-phase contrast microscope. We found that D increased at the beginning of the phase separation and tended to reach an equilibrium state, while the characteristic length scale ξ of the morphology increased monotonically with time according to a power law $\xi - t^\alpha$.

Introduction

Multicomponent polymer systems, the so-called polymer alloys, are designed to exhibit properties superior to their single components. Because the properties of polymer alloys strongly depend on their morphologies, the importance of controlling the morphology of multicomponent polymers has been widely recognized.[1,2] External fields such as shear flow[3] and electric fields (E-field)[4–13] have been used to modulate the morphologies so far. Those studies revealed that both the flow and the E-field could stretch, orient, and break up the phase-separated domains. Flows induce the transport and the deformation process of polymer chains to a large extent,[14] e.g., the macroscopic external deformation is directly reflected in the microscopic deformation of polymer chains under the affine deformation assumption. On the other hand, E-field can also orient the dipoles pendant on the polymer chain. However, the degree of orientation is very small because the realistic E-field strength is often limited within a few kV/cm due to the occurrence of electric discharge. Specifically, the average orientation angle $\langle\cos\theta\rangle$ of the dipole vector with respect to the E-field direction is simply estimated by the Langevin function, $L(\mu E/k_B T)$, defined as $L(x) = -1/x + \coth(x)$, where μ is the dipole moment, and k_B is the Boltzmann constant. If the electric field with the magnitude $E = 10$ kV cm^{-1} is applied to the dipole $\mu = 2$ D at $T = 300$ K, then $\langle\cos\theta\rangle$ is approximately 5.4×10^{-4}. From this estimation, one could conclude that the orientation or the conformational change of polymer chains is negligibly small and therefore the mixing free energy of the blends is almost unchanged through polymer chain deformation induced by an E-field. However, Reich and Gordon[15] reported a demixing process of polystyrene/ poly(vinyl methyl ether) blends induced by an E-field. A small shift of the critical temperature T_{critical} was observed and ascribed to the excess free-energy term due to the nonlinear concentration dependence of the dielectric constants of the blend. It is noted that induction of the large shift in T_{critical} by using an E-field is experimentally much harder than the case of shear field.[16–18]

If a two-component system is phase-separated, E-field gives rise to an electric stress at the interfaces between two phases. The magnitude of this stress depends on the difference in dielectric constants and/or conductivities.[19] It has been known that this stress can deform the phase-separated domains. However, this type of electric stress does not modulate the morphologies so easily compared to the flow field.[10,11] In spite of such difficulty for the morphology control, E-field is more preferential under some specific cases. For instance, to control the structure of thin films or small size devices consisting of components with different electric properties, the E-field is superior to the flow field because the former is more easily applied at a small spatial region.[20]

Concerning the utilization of an E-field, several studies have been already performed aiming at controlling the morphologies of both polymer blends[4–13] and block copolymers.[20–23] Those studies mainly examined immiscible (two-phase) systems. Among them, Krause et al.[7–11] made slightly different approaches: they applied an E-field for polymer/polymer/solvent ternary blends undergoing phase separation during the solvent-casting process at a constant temperature. In the process of solvent evaporation, the solvent content is not conserved and the mobility drastically changes, especially when the glass-transition temperature of the solution comes close to the experimental temperature. Therefore, it is difficult not only to examine the formation kinetics of the modulated phase but also to control the morphology in this particular case. From this viewpoint, much simpler systems are preferred such as phase-separating systems without changing the chemical compositions. For this reason, we examined in this study a blend that undergoes phase separation induced by a temperature jump from the one-phase into the two-phase region under an electric field. Our objective is to examine the following two points: (1) the effect of an E-field on the bicontinuous structure emerging near the critical composition and (2) the consequence of the coupling with the E-field on the coarsening and anisotropy of the resulting morphology.

Experimental Section

Samples. Poly(2-chlorostyrene) (P2CS)/poly(vinyl methyl ether) (PVME) blends are known to have a lower critical solution temperature (LCST).[24,25] We used this blend as a model system to examine the temperature-induced phase separation under an electric field. P2CS was synthesized by radical polymerization of 2-chlorostyrene with the weight-average molecular weight, $M_w = 4.42$

* Corresponding author. E-mail address: urakawa@ chem.sci.osaka-u.ac.jp. Telephone: +81-6-6850-5458. Fax: +81-6-6850-5538.
† Technology & Information Promotion Division JST "CREATE" Osaka, Osaka Science and Technology Center, 2-7-1 Ayumino, Izumi, Osaka 594-1157, Japan.
‡ Department of Macromolecular Science, Graduate School of Science, Osaka University, 1-1 Machikaneyama-cho, Toyonaka, Osaka 560-0043, Japan.
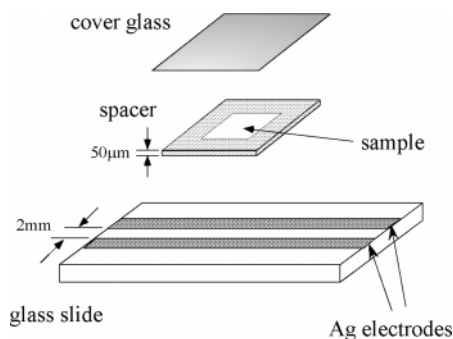
Figure 1. Schematic illustration of the electrodes used to apply electric fields to the samples.

$\times 10^5$ g mol^{-1} as determined by intrinsic viscosity. PVME (Polymer Source Inc.) has $M_w = 1.04 \times 10^5$, as also determined by the intrinsic viscosity. A small amount of lithium perchlorate (LiClO$_4$, Wako Chemicals) was added into the blends to enhance the response to an E-field.

Polymer blends with and without LiClO$_4$ were prepared by casting their cyclohexanone solutions and subsequently dried under vacuum at 80−100 °C. This range of temperature is in the one-phase region between the glass-transition temperature and the cloud points.

We mainly investigated P2CS/PVME blends with the composition 30:70 throughout the study. The content of LiClO$_4$ was fixed at 0.5 wt %.

Electric Field Generator and the Shape of Electrodes. Sinusoidal voltages with a fixed frequency of 10 Hz were generated by a function generator (AG-203, Kenwood) and amplified by a voltage amplifier (HOPP-3B1, Matsusada Precision) up to 1.5 kV (amplitude) at maximum. We applied the amplified voltage to the sample and monitored its magnitude by using a standard resistance connected parallel to the sample electrode.

The electrodes were made by silver vapor-deposited onto glass slides, as schematically shown in Figure 1, together with its dimension. The thickness of the deposited electrodes was less than 0.2 μm, and the sample thickness was adjusted at 50 μm using a Teflon spacer. Because of such thin electrodes, the electric field in the sample would be nonuniform. According to Tsori et al.[13] such a nonuniform E-field (field gradient) could induce the phase separation. However, in this study we could not observe such a field-gradient-induced phase separation. Furthermore, for the blends containing LiClO$_4$, there was no clear position dependence between two electrodes in the morphologies emerged by temperature-induced phase separation under an E-field. Therefore, we basically ignored the effect of nonuniformity in the field strength. The observation of the morphologies was made at three positions, i.e., near the two electrodes and the central part, and the spatial uniformity of the resulting morphology was checked every time.

Observation of the Time-Evolution of Morphology. We observed phase separation after a temperature jump (T-jump) from the one phase into the unstable region with a shallow quench depth (about 0−5 °C). The sinusoidal (AC) electric field with the frequency 10 Hz was applied to the sample in the miscible region just before the T-jump. In this study, we did not made in situ observation of the morphology under an electric field because of the experimental difficulty. After a certain time, the sample was quickly cooled down to room temperature (25 °C) and the morphology was observed under a phase-contrast optical microscope (Nikon, model E400) using a 100× oil immersion objective. During the duration time of optical microscopy (about 5 min) at room temperature, the change in the morphology was not observed. The thermal history of the blends is schematically drawn in Figure 2.

The images of the resulting morphologies observed with a phase-contrast optical microscope were taken by using a CCD camera (Hamamatsu, C2400) and a video capture board (Scion Corporation, LG-3). We analyzed the digitized images by using two-dimensional
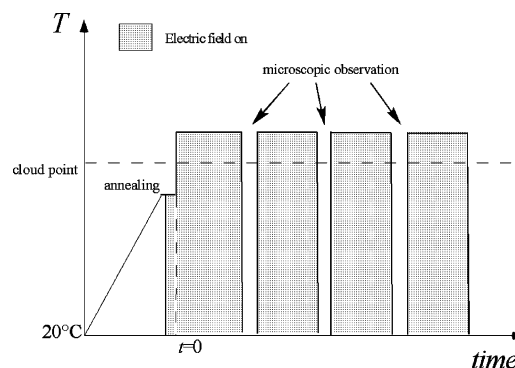

Figure 2. Schematic representation of the thermal and E-field application history of the blend. For the immersion oil optical microscopy, the sample was quenched after a certain period of time.
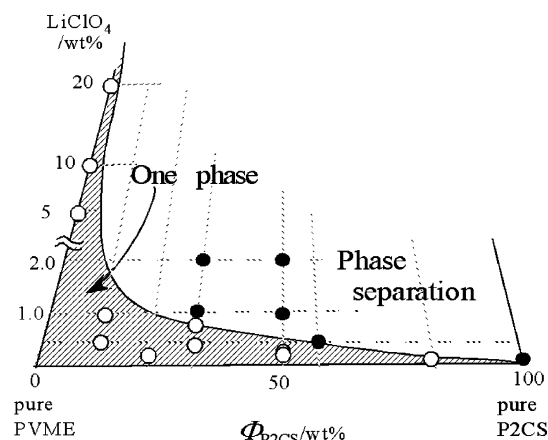

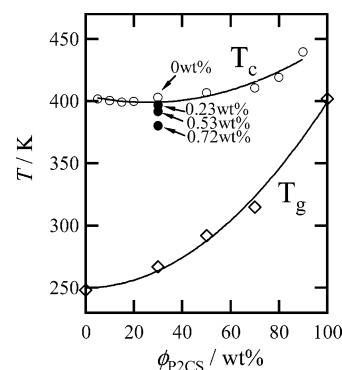**Figure 3.** Phase diagram of the ternary system, P2CS/PVME/LiClO$_4$ at 25 °C.

Figure 4. Composition dependences of the cloud points T_c and the glass transition temperatures T_g for the P2CS/PVME blend. The variation of T_c with the LiClO$_4$ concentration (relative to the total polymer weights) are indicated by the filled circles at the blend composition $\phi_{P2CS} = 30$ wt %.

fast Fourier transform (2D-FFT) with a standard software for image analysis (Scion Images).

Results

Phase Diagrams of P2CS/PVME/LiClO$_4$. The phase behavior of P2CS/PVME blends was previously reported.[24,25] However, the phase behavior of a ternary system (P2CS/PVME/LiClO$_4$) was not available. Therefore, we roughly examined the miscibility by eyes or by optical microscope observation whether the blends were opaque or not at room temperature (25 °C). The results are summarized in Figure 3 as the ternary component phase diagram. It is found that the addition of LiClO$_4$ reduces the miscibility of the blend.
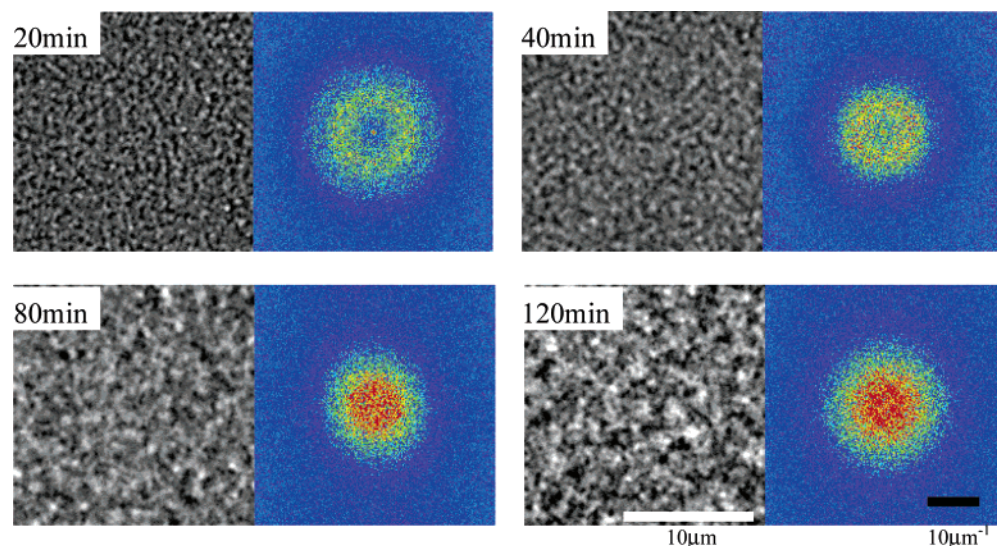
Figure 5. Time-evolution of phase-separated structures and the corresponding 2D-FFT images observed for a P2CS/PVME (30:70) in the absence of an electric field at 134 °C.

Phase separation was induced at relatively high temperature to achieve the visible deformation of the phase-separated domains. In this work, we chose LiClO$_4$ concentration 0.5 wt % with respect to the total mass of polymers and the polymer composition 30:70 (= P2CS/PVME) as a critical composition.

Figure 4 shows the phase separation temperatures (cloud points) T_c's and glass transition temperatures T_g's as a function of the blend composition. In this figure, the change of T_c with the addition of LiClO$_4$ is also indicated by the filled circles for the P2CS/PVME (30:70) blend.

Morphologies of P2CS/PVME Blends in the Absence of an Electric Field. First, we examined the phase separation of P2CS/PVME (30:70) mixture without LiClO$_4$ in the absence of an E-field. The blend was annealed at 110 °C (below T_c) for 30 min and then destabilized at 134 °C (4 °C above T_c). Figure 5 shows the morphologies observed at various elapsed times after the T-jump. As seen here, the typical isotropic interconnecting (bicontinuous) structures clearly appear.

The 2-dimensional Fourier transform (2D-FFT) spectra are also illustrated in this figure. The circular FFT power spectra ensure the isotropy of the morphology. It is worth noting that, although T_c of the blend decreases with adding 0.5 wt % LiClO$_4$, the change in the morphology was not significant.

Phase Separation in the Presence of an Electric Field. *Spatial Inhomogeneity in the Morphology Observed between the Two Electrodes.* For P2CS/PVME (30:70) blends without LiClO$_4$, we found that the application of an AC electric field induced spatial inhomogeneity in the morphology between the two electrodes. In the central part between the two electrodes, isotropic morphologies similar to those shown in Figure 5 was observed, even for a long annealing time in the unstable region. However, modulated structure was observed in the vicinity of two electrodes, at least within a 30 μm distance from the edge of the electrodes. The morphologies observed at three positions (near the upper side electrode, middle part, and near the lower side electrode) are shown in Figure 6a (from the top to the bottom, respectively). The gap of the two electrodes is about 2 mm. The edge of the one electrode is located at the top edge of the top picture and the other one is located at the bottom edge of the bottom picture. It was found that the phase-separated domains are partially oriented along the direction of the E-field in the vicinity of two electrodes (top and bottom images).
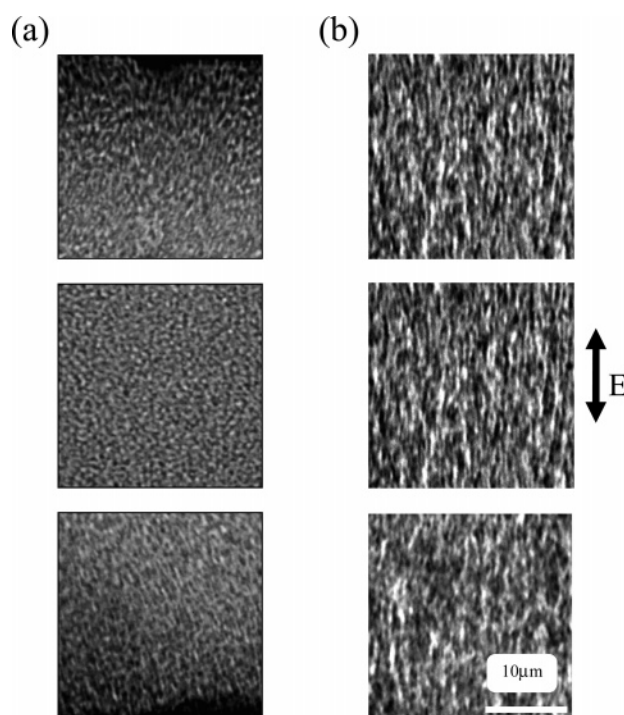

Figure 6. Phase-contrast optical micrographs observed for a P2CS/PVME (30:70) with (a) 0 wt % and (b) 0.5 wt % LiClO$_4$ at three different positions of the electrodes: near the upper electrode (top), central part (middle), and near the lower electrode (bottom). The E-field strength (amplitude) and the frequency were 11.2 kV/cm and 10 Hz, respectively.

On the other hand, we found that the addition of 0.5 wt % LiClO$_4$ could drastically change the emerging morphologies. As an example, Figure 6b shows the optical micrographs observed at the three similar positions after 80 min phase separation at $T = 118$ °C. It is obvious that all the morphologies are uniformly deformed and oriented parallel to the E-field direction. As mentioned in the Discussion Section, the conductivity difference between two phases plays an important role for the morphological change under an E-field. Moreover, we see that the effect of an E-field is not significant at the beginning of the phase separation. Time dependence of the structure change is described in detail in the next section.
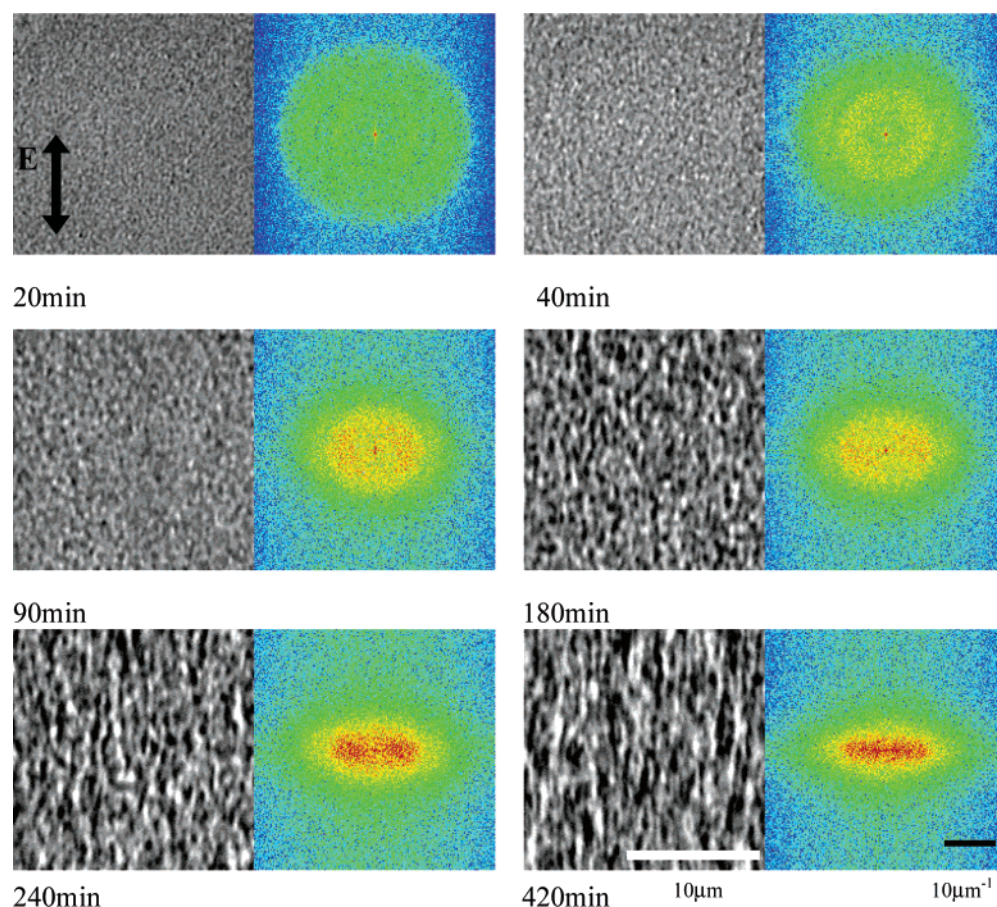
Figure 7. Time-evolution of phase-separated structures and corresponding 2D-FFT power spectra obtained for a P2CS/PVEM (30:70) blend containing LiClO$_4$ (0.5 wt %) under an electric field (AC 11.2 kV/cm, $f = 10$ Hz) at 118 °C.

Time-Evolution of the Morphology under an E-Field. As a typical example, Figure 7 shows the time course of the phase-separated morphologies observed for a P2CS/PVME (30:70) blend containing 0.5 wt % LiClO$_4$ under an AC E-field (11.2 kV/cm, 10 Hz) along with the corresponding 2D-FFT power spectra. These pictures were taken at the central part between the two electrodes. As mentioned in the previous section, similar morphologies appeared at any positions between the two electrodes.

It is obvious from these data that, in the early stage of the phase separation, the structure was almost isotropic, as evidenced by the shape of the 2D-FFT power spectra. However, as the phase separation proceeded, the morphology turned anisotropic and coarsened with time. The change of 2D-FFT spectra also indicates these features: the size of the circular or ellipsoidal pattern gradually decreased, suggesting the increase in the characteristic length scale for the phase-separated morphology. At the same time, the isotropic → anisotropic transition can be also clearly observed through the change with time in the shape of the 2D-FFT power spectra from circular to ellipsoidal shape.

Discussion

Effect of LiClO$_4$ on the Uniform Deformation of the Morphology. Electric and hydrodynamic stresses acting at the domain interfaces between P2CS-rich and PVME-rich phases would be the origin of this structure deformation. Because of the difference in the dielectric constants between the two phases, only the electric stress perpendicular to the interface is generated. However, if there is a conductivity difference between two phases, the tangential electric stress parallel to the interface would be created at the same time.[19] As a result, flow is generated around the interfaces, and then hydrodynamic stress induced by the flow could deform the phase-separated domains. In addition, we think that the interfacial polarization arising from the conducting species, which are charged up at the phase-separated interfaces, may play an important role for the generation of a large electric stress. Tsori et al. suggested that the presence of ions (conductivity contrast) could induce strong orienting forces on the microphase segregated block copolymers.[23]

Upon phase separation, the LiClO$_4$ component preferentially dissolves in the PVME-rich domain, judging from the phase behavior shown in Figure 3. As a rough estimation, the conductivity σ of the PVME/LiClO$_4$ (0.5 wt %) mixture is on the order of 10^{-7}–10^{-8} S cm^{-1} at 118 °C[26] and that of P2CS, which can hardly dissolve LiClO$_4$, is about 10^{-10} S cm^{-1}.[25] The difference in these σ (2–3 orders magnitude difference) will be the maximum expected for the completely immiscible case. In this phase-separated blend, the compositions of each phase do not differ so much, however, there is no doubt that the two phases have different conductivities.

It is speculated that, without LiClO$_4$, a trace of conducting impurity emerging from the electrodes can result in the anisotropic morphology in the vicinity of the electrodes shown in Figure 6b. Probably the electric stress caused by the difference in dielectric constants is very weak in this particular case so that the isotropic morphology will appear in the central part between the two electrodes. However, for a blend containing LiClO$_4$, because the salt is distributed uniformly in the sample, the morphology is uniformly deformed.

Characteristic Length Scale and the Structural Anisotropy. The characteristic length scale of the morphology was
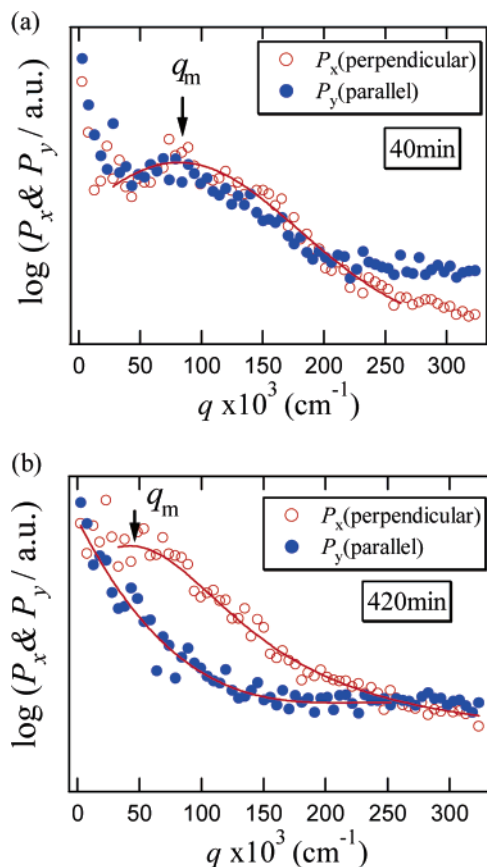
Figure 8. Sector-averaged 2D-FFT intensities $P_x(q)$ and $P_y(q)$ for a P2CS/PVME/LiClO$_4$ blend after (a) 40 min and (b) 420 min phase separation under the AC electric field ($E_0 = 11.2$ kV/cm, $f = 10$ Hz) at 120 °C.

determined from the 2D-FFT power spectra. Parts a and b of Figure 8 show the wave number (q) dependence of the intensities P_x and P_y averaged over a sector in the angle width of 10° along the direction perpendicular (x) and parallel (y) to the E-field, respectively, for different times. At $t = 40$ min after the T-jump, the P_x and P_y exhibit similar profiles, reflecting the isotropic morphology. As time elapses, the morphology becomes aniso-tropic and Fourier intensities at the two directions behave differently. For example, at $t = 420$ min after a T-jump, the peak position q_m of P_x remains in the same q range, whereas P_y no longer shows a peak. From the q_m of P_x, we determined the average characteristic length scale ξ_x perpendicular to the E-field direction. Figure 9 shows the time dependence of ξ_x under various E-field strengths. It can be seen that the effect of E-field is not significant for the ξ_x values. This may be because E-field dose not induce a large electric stress at the interface perpendicular to the field direction (x-direction), and thus the interface periodicity in the x-direction will be less affected by the E-field.

Even through the data scatter, all the $\xi_x(t)$ were fitted with the power law equation:

$$\xi_x(t) = \xi_{x,0} t^\alpha \quad (1)$$

Here $\xi_{x,0}$ and α are the constants. The numerical values of α are shown in the legend of the figure. We can see that α takes the values around 0.5. These α values are consistent with the literature data for PS/PVME blends near the critical composi-tion[27] if the observed phase separation can be categorized as in the late stage (in this case, typical α values were in the range of 0.5−1).
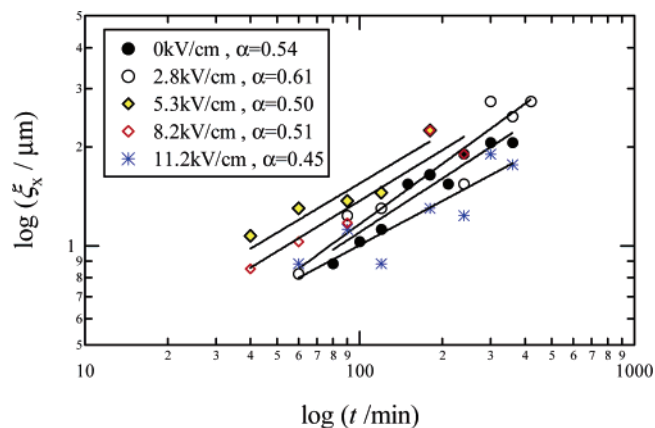

Figure 9. Time-evolution of characteristic length scale ξ_x, in the direction perpendicular to the E-field.

To quantitatively evaluate the morphology anisotropy, we define the anisotropy parameter, D, from the 2D-FFT images by using the following equation:

$$D = \frac{\displaystyle\sum_{q_x,q_y} \frac{q_y^2 - q_x^2}{q^2} P(q_x,q_y)}{\displaystyle\sum_{q_x,q_y} P(q_x,q_y)} \quad (2)$$

Here q_x,q_y are the components of the wave vector **q** with $\mathbf{q}^2 = q_x^2 + q_y^2$. $P(q_x, q_y)$ is the intensity of the 2D-FFT spectrum. The anisotropy parameter defined by eq 2 corresponds to the (normalized) form birefringence introduced by Onuki and Doi.[28] For example, in the case where the interfaces perfectly align parallel (or perpendicular) to the field (y-axis) direction, D becomes 1 (or −1). On the other hand, D becomes zero for perfect isotropic structures.

Figure 10a shows the time dependence of D with several electric field strengths. It was found that D for $E_0 \geq 5.3$ kV/cm increases at short time and tends to saturate at long time. We can qualitatively understand this behavior by considering the competition between two factors: the interfacial force and electric stress. The interfacial force tends to form isotropic structure, which opposes the electric stretching force along the field direction. Similar behavior was well-known for the deformation of a droplet suspended in the viscous media in the presence of an E-field. In that case, the degree of deformation is defined as $(Y - X)/(Y + X)$, where X and Y are the lengths of the long and short axes of the deformed droplet, respectively.[5] The equilibrium deformation is known to be proportional to the square of the field strength E^2. Although the deformation mechanism of the bicontinuous structure in the presence of an E-field is not known, it is interesting to examine the E dependence of D by the analogy with the droplet deformation mechanism. Figure 10b shows the double logarithmic plot of D vs E. The slope of this plot is approximately 2, suggesting that the equilibrium value of D is proportional to E^2.

By comparing Figures 9 and 10a, it is found that at the late stage of phase separation, ξ continues increasing while D approaches a constant value. This indicates that the degree of anisotropy for the phase-separated domains does not develop in accordance with the structural coarsening process.

The detailed mechanism for the deformation of the bicon-tinuous morphology induced by an E-field is currently under investigation.
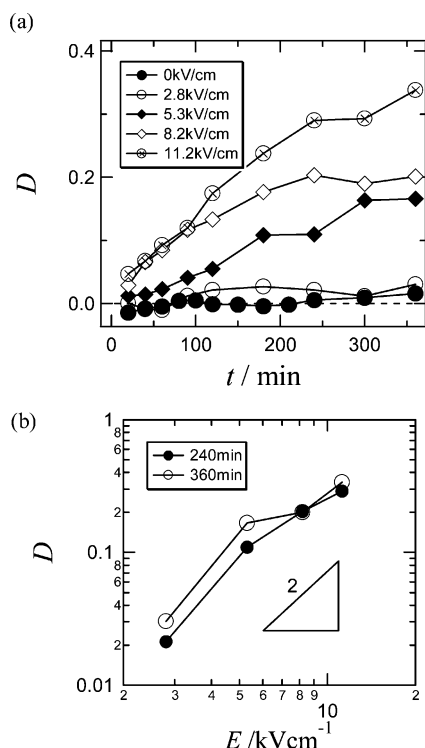
Figure 10. (a) Time dependence of the anisotropy parameter, D, evaluated from the FFT power spectra of a P2CS/PVME (30:70) blend containing LiClO$_4$ (0.5 wt %). (b) Dependence of the equilibrium D obtained at $t = 240$ and 360 min on the electric field strength.

Conclusion

We observed the time-evolution process of the deformed and oriented morphologies induced by a temperature jump under an AC electric field. One of our findings is that addition of a trace (0.5 wt %) of LiClO$_4$ into the P2CS/PVME (30:70) blends results in the formation of a uniform bicontinuous structure oriented parallel to the E-field between the two electrodes.

The characteristic length scale ξ_x increased monotonically with a power law $\xi_x - t^\alpha$, where not only the ξ_x but also the α values were not significantly affected by the E-field strength. On the other hand, the degree of anisotropy D of the phase-separated structures was a monotonically increasing function of the field strength E. Unlike ξ_x, which keeps increasing with time, D first increases with increasing time and eventually approaches a constant. This constant D value was approximately proportional to the square of the E-field strength.

References and Notes

(1) Hsu, W. Y.; Wu, S. *Polym. Eng. Sci.* **1993**, *33*, 293−302.
(2) Imagawa, A.; Tran-Cong, Q. *Macromolecules* **1995**, *28*, 8388−8394.
(3) Han, C. C.; Yao, Y.; Zhang, R.; Hobbie, E. K. *Polymer* **2006**, *47*, 3271−3286.
(4) Moriya S.; Adachi K.; Kotaka T. *Polym. Commun.* **1985**, *26*, 235−237.
(5) Moriya, S.; Adachi, K.; Kotaka, T. *Langmuir* **1986**, *2*, 155−160.
(6) Moriya, S.; Adachi, K.; Kotaka, T. *Langmuir* **1986**, *2*, 161−165.
(7) Xi, K.; Krause, S. *Macromolecules* **1998**, *31*, 3974−3984.
(8) Venugopal, G.; Krause, S.; Wnek, G. E. *J. Polymer Sci., Part C: Polym. Lett.* **1989**, *27*, 497−501.
(9) Venugopal, G.; Krause, S. *Macromolecules* **1992**, *25*, 4626−4634.
(10) Venugopal, G.; Krause, S.; Wnek, G. E. *Chem. Mater.* **1992**, *4*, 1334−1343.
(11) Serpico, J. M.; Wnek, G. E.; Krause, S.; Smith, T. W.; Luca, D. J.; Van, Laeken, A. *Macromolecules* **1991**, *24*, 6879−6881.
(12) Winoto, D.; Carr, S. H. *Macromolecules* **1996**, *29*, 5149−5156.
(13) Tsori, Y.; Tournilhac, F.; Leibler, L. *Nature* **2004**, *430*, 544−547.
(14) Larson, R. G. *Rheol. Acta* **1992**, *31*, 497−520.
(15) Wirtz, D.; Fuller, G. G. *Phys. Rev. Lett.* **1993**, *71*, 2236−2239.
(16) Hindawi, I. A.; Higgins, J. S.; Weiss, R. A. *Polymer* **1992**, *33*, 2522−2529.
(17) Murase, H.; Kume, T.; Hashimoto, T.; Ohta, Y.; Mizukami, T. *Macromolecules* **1995**, *28*, 7724−7729.
(18) Fernandez, M. L.; Higgins, J. S.; Horst, R.; Wolf, B. A. *Polymer* **1995**, *36*, 149−154.
(19) Torza, S.; Cox, R. G.; Mason, S. G. *Philos. Trans. R. Soc. London, Ser. A* **1971**, *269*, 295−319.
(20) Morkved, T. L.; Lu, M.; Urbas, A. M.; Ehrichs, E. E.; Jaeger, H. M.; Mansky, P.; Russel, T. P. *Science* **1996**, *273*, 931−933.
(21) Amundson, K.; Helfand, E.; Davis, D. D.; Quan, X.; Patel, S. S.; Smith, S. D. *Macromolecules* **1991**, *24*, 6546−6548.
(22) Amundson, K.; Helfand, E.; Quan, X.; Smith, D. S. *Macromolecules* **1993**, *26*, 2698−2703.
(23) Tsori, Y.; Tournilhac, F.; Leibler, L. *Macromolecules* **2002**, *36*, 5873−5877.
(24) Tran-Cong, Q.; Nakano, H.; Okinaka, J.; Kawakubo, R. *Polymer* **1994**, *35*, 1242−1247.
(25) Urakawa, O.; Fuse, Y.; Hori, H.; Tran-Cong, Q.; Yano, O. *Polymer* **2001**, *42*, 765−773.
(26) Zhang, S.; Runt J. *J. Phys. Chem. B* **2004**, *108*, 6295−6302.
(27) Hashimoto, T.; Itakura, M.; Shimidzu, N. *J. Chem. Phys.* **1986**, *85*, 6773−6786.
(28) Onuki, A.; Doi, M. *J. Chem. Phys.* **1986**, *85*, 1190−1197.